Thermodiffusion in positively charged magnetic colloids: Influence of the particle diameter

A. L. Sehnem
Instituto de Física, Universidade de São Paulo, São Paulo, Brazil

R. Aquino and A. F. C. Campos
Faculdade UnB–Planaltina, Universidade de Brasília, Brasília, Distrito Federal, Brazil

F. A. Tourinho
Instituto de Química, Universidade de Brasília, Brasília, Distrito Federal, Brazil

J. Depeyrot
Instituto de Física, Universidade de Brasília, Brasília, Distrito Federal, Brazil

A. M. Figueiredo Neto
Instituto de Física, Universidade de São Paulo, São Paulo, Brazil
(Received 6 December 2013; published 24 March 2014)

The Soret coefficient (S_T) of positively charged magnetic colloids was measured as a function of the nanoparticles' diameter. The Z-scan technique and the generalization of the thermal lens model proved to be a reliable technique to measure S_T. We show that S_T is negative and increases with the particle's diameter, being best described by a functional dependence of the type $S_T \propto d_0$. Potentiometric and conductometric experiments show that the particle's surface charge decreases as the temperature increases, changing the electrostatic interaction between the nanoparticles. The temperature gradient imposed in the ferrofluid by the Gaussian laser beam leads to the formation of the particle's concentration gradient. The origin of this phenomenon is discussed in terms of the decrease of the particle's surface charge in the hottest region of the sample and the thermoelectric field due to the inhomogeneous distribution of hydrogenous ions present in the colloidal suspension.

DOI: 10.1103/PhysRevE.89.032308 PACS number(s): 82.70.Dd, 47.57.jd, 66.10.cg

I. INTRODUCTION

The phenomenon of thermodiffusion is an interesting subject of fundamental research in the physics of complex fluids. When a mixture is subjected to a temperature gradient, an inhomogeneous distribution of the different components of the mixture takes place. The discovery of this effect is due to Charles Soret, who observed this inhomogeneity in saline solutions subjected to a temperature gradient [1]. Since then, many different molecular mixtures and colloidal systems have been shown to exhibit this effect, which is known as the Soret effect. Although this effect has been known for more than a century, a microscopic description of the phenomenon is still lacking, and it seems to be dependent on the particular system under investigation.

Let us consider the case of a solution with one solute and a solvent. It is known that the interactions between solute and solvent play a key role in thermodiffusion for most complex fluids [2]. At a given temperature gradient $\vec{\nabla}T$, the solute mass flow $\vec{J}_M$ is described through Eq. (1) [3,4]:

$$\vec{J}_M = -D_M(\vec{\nabla}\Phi + S_T\Phi\vec{\nabla}T), \tag{1}$$

where D_M, $\vec{\nabla}\Phi$, S_T, and Φ are the translational mass diffusion coefficient, the solute concentration gradient, the Soret coefficient, and the solute volume concentration, respectively. S_T is defined as the ratio between the coefficient of thermal diffusion D_T and D_M [5,6]: $S_T = D_T/D_M$. It couples the concentration and temperature gradients and assumes positive (negative) values when the solute particles move to the cold (hot) region of the sample. Systems with $S_T > 0$ ($S_T < 0$) exhibit thermophobic (thermophilic) behavior [7].

Complex fluids, which comprise a broad range of systems (e.g., liquid crystals, polymers, colloids, and electrolyte solutions), are prime candidates to demonstrate thermodiffusion [8–14]. Magnetic colloids, also called ferrofluids (FFs), consist of magnetic nanoparticles (typically 10 nm in diameter) suspended in an appropriate carrier fluid [15]. Two types of FFs are known, namely charged and surfacted. They differ with regard to the strategy employed to maintain colloidal stability. In the case of ionic FFs, particles are electrically charged; in surfacted FFs, they are coated with surfactant molecules. Interestingly, one of the most promising applications of FFs is in biomedicine [16].

The investigation of the Soret effect in FFs revealed interesting results. The possibility of controlling the size, shape, surface charge, and coating of the particles opens these systems to a rich field of research on thermodiffusion in different experimental conditions. Alves *et al*. [7] showed that the sign of S_T for these materials depends on the particles' surface characteristics. To put in evidence the influence of the particle and solvent and the interparticle interactions on thermodiffusion, Mériguet *et al*. [17] reported experiments on S_T as a function of particle concentration and ionic strength. It was found that interparticle interactions have a significant influence on S_T for $0 < \Phi < 10\%$, while variations in ionic strength do not change S_T at an infinite dilution limit, as in the case of sodium dodecyl sulfate micelles in water [18]. Mezulis *et al*. [19] observed that S_T does not significantly vary with increasing ion concentration in electrostatically

stabilized ferrofluids. To the best of our knowledge, there are no systematic experimental results about an eventual dependence of S_T with the size of the FF particles. Even for nonmagnetic colloids, such as polystyrene nanoparticles in an aqueous medium, controversial results were reported [20–22]. Duhr and Braun [20] reported a dependence of S_T with the particles' diameter d of the type $S_T \propto d^2$, while other experiments [21,22] revealed a dependence of the type $S_T \propto d$.

In this work, we investigate the Soret coefficient amplitude dependence with particle mean size in acidic ferrofluids. The optical Z-scan (ZS) technique [23] is used to obtain the Soret coefficient. The results will be discussed taking into account changes in the particle's surface charge due to the temperature gradient. The paper is organized as follows: in the experiment section, the sample characteristics and the ZS apparatus details are given; afterward, the effect of temperature in the particle's surface charge (σ) is discussed on the basis of the measurement σ as a function of the sample's pH and temperature. The methodology for ZS data acquisition and analysis is presented, followed by the results and discussion section, and finally the conclusion.

II. EXPERIMENT

A. Magnetic colloidal solutions

The synthesis of the magnetic nanocolloids based on cobalt ferrite was made according to procedures described elsewhere [24]. Alkaline hydrothermal coprecipitation of 1:2 mixtures of Co^{2+} and Fe^{3+} salt solutions performed in different pH and reagent addition rates allowed us to control the mean size of the nanoparticles [25,26]. A chemical treatment of the particles' surface with a solution of 1 mol/L of $Fe(NO_3)_3$ at 100 °C creates a protective maghemite shell around the $CoFe_2O_4$ core [26]. Then, the nanoparticles are dispersed in an aqueous acidic medium, remaining at a stable and homogeneous sol phase solution thanks to their surface charge and convenient adjustment of ionic strength. The FF magnetic nanoparticles are dispersed in water at pH $\sim$ 3. The sizes of the nanoparticles were measured with transmission electron microscopy (TEM). The particle diameter (d) distribution functions were described by a log-normal function: $P(d) = \frac{1}{\sqrt{2\pi}d\sigma_d}\exp(-\frac{\ln^2(d/d_0)}{2\sigma_d^2})$, where d_0 and σ_d are the mean value of the diameter and the standard deviation. Solutions were labeled as FFi, with $i = 1-5$. Absorption measurements were performed at a uv/vis spectrophotometer (UNICO 2800), with the sample inserted into an 80 μm thickness cuvette. The volume fraction of the samples used in our experiments was $\Phi = 0.15\%$. This concentration was chosen such that a good signal-to-noise ratio is observed in the ZS experiment. Details about the dispersions are given in Table I.

B. The Z-scan apparatus

Details about the ZS apparatus can be found in [23]. The beam power was chosen to be such a value that all samples furnished the same thermal-lens phase amplitude $C_T \sim -0.06$ [see Eq. (4) in the following]. This value is low enough to avoid spherical aberration effects [27].

TABLE I. Values of the mean particle sizes d_0 obtained by TEM and log-normal standard deviation σ_d; values of the measured absorption coefficient α and respective beam power P applied in order to get about the same thermal lens amplitude.

Sample	d_0 (nm)	σ_d	α (cm^{-1})	P (mW)
FF1	3.2	0.2	89.2	2.95
FF2	4.2	0.2	57.3	4.60
FF3	8.0	0.2	135.0	1.94
FF4	9.0	0.1	96.4	2.70
FF5	13.6	0.2	105.0	2.50

In the ZS experiment, we use a cw doubled-frequency Nd:YVO_4 ($\lambda = 532$ nm) laser, with a Gaussian intensity profile. A mechanical shutter does the time modulation of intensity with top-hat pulses of equal duration, $\Delta t = 20$ s. The Gaussian beam is focused by a lens with focal length $f = 100$ mm, providing a beam waist of $\omega_0 = 24.3$ μm and Rayleigh length $z_0 = (\pi\omega_0^2/\lambda) = 3.24$ mm. The sample is placed in a holder made of two flat optical glasses in slab geometry (sample thickness of 80 μm), positioned on a chart that moves the ensemble along the z axis, as controlled by a computer. Software records the light transmittance acquired by an oscilloscope connected to the far-field detector. The acquisition rate of the oscilloscope is $\sim$100 Hz. We worked in the closed aperture geometry of the ZS experiment, with an iris in the front of the detector.

III. EFFECT OF TEMPERATURE IN THE PARTICLE'S SURFACE CHARGE

In electrostatically stabilized ferrofluids, colloidal stability is governed by the chemical equilibrium of the protonation and deprotonation reactions at the particle's surface. These reactions give rise to superficial particle sites that correspond to transition-metal ions, which can undergo an aquation reaction according to the schematic equilibrium depicted in the following:

$$\equiv M^{n+} + H_2O \rightleftharpoons \equiv M,H_2O^{n+},$$

where M represents the metallic ion at the surface. Thus, the reactions

$$\equiv MOH_2^{+} + H_2O \overset{pK_1}{\rightleftharpoons} \equiv MOH + H_3O^{+},$$
$$\equiv MOH + H_2O \overset{pK_2}{\rightleftharpoons} \equiv MO^{-} + H_3O^{-},$$

are responsible for the formation of the surface charge of the particles in the liquid solution [28]. The particle surface behaves like a weak diprotic Brönsted acid leading, through the above acid-base equilibriums, to three kinds of superficial sites where most of them are $\equiv MOH_2^+$ in a strong acidic medium, $\equiv MO^-$ in a strong basic medium, and $\equiv MOH$, the intermediate amphoteric sites, at the point of the zero-charge region. As these reactions have independent equilibrium constants pK_1 and pK_2, we may estimate the number of positive and negative charges at the surface of the particles. The two equilibrium constants are obtained with simultaneous potentiometric and conductometric experiments [28,29]. The surface charge of the nanoparticles is calculated as a function

of the equilibrium constants and the pH of the solution with the expression

$$\sigma\ (\mathrm{pH}) = \frac{FV}{a}\left(\frac{10^{-2\,\mathrm{pH}} - 10^{-(pK_1+pK_2)}}{10^{-2\,\mathrm{pH}} - 10^{-(\mathrm{pH}+pK_1)} + 10^{-(pK_1+pK_2)}}\right)C,$$

where F is the Faraday constant, V is the volume of the suspension (nanoparticles + carrier fluid), a is the total surface area of the nanoparticles, and C is the concentration of the surface sites. Another parameter that changes the chemical equilibrium in the particle's surface is the temperature. The heating of the sample shifts the equilibrium, inducing ionization or dissociation of surface sites. As we could make a good estimate of the temperature increase in the ZS experiment, we use the procedure described above to determine the surface charge in a sample maintained at 30 °C and in another sample at room temperature, 23 °C. The potentiometric and conductometric curves were obtained using the well-established titration method [28]. The samples are initially at pH = 2.0 and, titration with a solution 0.1 mol/L of NaOH changes the ionic strength of the solution. Curves of pH and conductivity as a function of the titrant volume were obtained and the equilibrium constants were calculated from these curves [28]. Figure 1 shows the results for surface charge in two temperatures, 23 and 30 °C for the biggest nanoparticles (solution FF5). As can be seen, for pH $\leq$ 2.6 and pH $\geq$ 11.5, the particle surface charge reaches its saturation value σ_{sat} since the superficial density of charge is no longer varying. This means that pH variations below 2.6 and above 11.5 do not affect the nanoparticle charge. Then, both curves were normalized by σ_{sat} at $T = 23$ °C. Analyzing the temperature dependence of σ_{sat}, we found that it decreases as the temperature increases. In other words, at the same pH the number of charged surface sites decreases as the temperature increases. Since our titration procedure starts from an acidic medium, this nanoparticle charge reduction is due to the process of dissociation of positive surface sites according to the protonation and deprotonation equilibrium equations. Similar results were reported by Mustafa and co-workers for alumina nanoparticles dispersed in water with KNO_3 as background electrolyte [30].

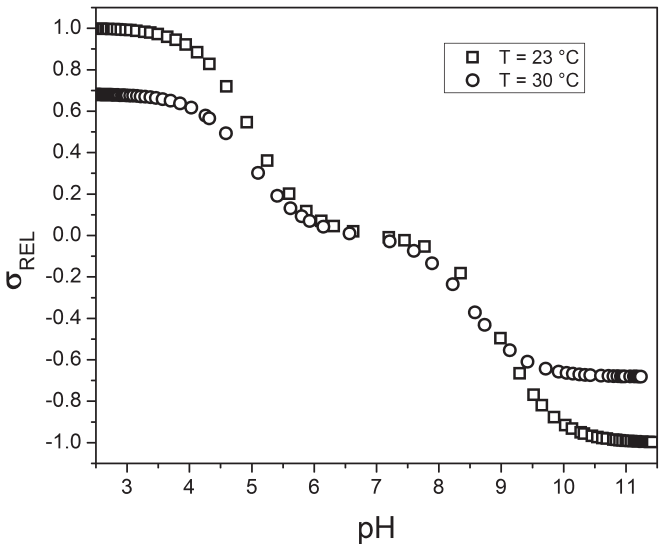

FIG. 1. Particles' surface charge as a function of the pH of the colloidal solution at two temperatures. The results are normalized with respect to the saturation value of σ at pH = 2.6 and $T = 23$ °C. Sample FF5.

IV. METHODOLOGY FOR ZS DATA ACQUISITION AND ANALYSIS

A thermal lensing model is usually applied for low absorption materials [31]. As ferrofluids are materials with high light absorption, the induced thermal lens should respect the limitation for spherical aberration. This is done in the ZS experiments limiting the incident beam power. The characteristic time of heat diffusion is written as $t_c = \omega^2/(4D_{\mathrm{th}}) = \omega^2\rho c_p/(4k)$, where k, ρ, and c_p are the thermal conductivity, mass density, and specific heat of the sample, and ω is the z-dependent beam radius in a ZS experiment. In our experimental conditions, $t_c = \sim 2$ ms. The characteristic time of the Soret effect is written as $t_{\mathrm{so}} = \omega^2/(4D_M)$, which, in our case, varies between 1.5 and 5 s (z-positions around the valley of the ZS curve). To assure that the Soret effect achieved its saturation, we fixed the pulse width at $\Delta t = 20$ s in the ZS experiment. During this time interval, the sample temperature in the center of the laser beam ($r = 0$) exhibited an increase of about 6 K with respect to that at the border of the beam, which gives a temperature gradient $\nabla T < 0.03$ K/μm. We verified that this value is not enough to generate convection in the sample.

Alves *et al.* proposed a generalization of the thermal lens model to include both the electronic nonlinear and Soret effects [23]. As the ZS experiment is accomplished with light pulses of $\Delta t = 20$ s, the electronic nonlinear, thermal, and Soret lenses are formed. Thus, the total change in the refractive index is

$$\delta n(r,t) = \frac{\partial n}{\partial I}\delta I(r,t) + \frac{\partial n}{\partial T}\partial T(r,t) + \frac{\partial n}{\partial c}\delta c(r,t), \qquad (2)$$

where the first, second, and third terms in Eq. (2) represent the electronic nonlinear, thermal, and Soret contributions. The transmittance $\Gamma(z,t)$ measured by the detector may be written as [23]

$$\Gamma(z,t) = \frac{\Gamma'}{1 - 2\gamma A + (1+\gamma^2)A^2},$$
$$A = \frac{C_s}{1+\gamma^2}\left(\frac{2t}{2t + t_{\mathrm{so}}}\right) + \frac{C_T}{1+\gamma^2} + \frac{C_N}{(1+\gamma^2)^2}, \qquad (3)$$

where the Soret C_s, thermal C_T, and electronic nonlinear C_N lens amplitudes are written as

$$C_s = -\frac{0.24b\alpha P\Phi S_T(\partial n/\partial c)}{k\lambda},$$
$$C_T = \frac{0.24b\alpha P(\partial n/\partial T)}{k\lambda}, \qquad (4)$$
$$C_N = -\frac{8bz_0 P(\partial n/\partial I)}{\pi\omega_0^4},$$

with $\gamma = z/z_0$, b is the sample thickness, and Γ is the transmittance at $z \gg z_0$.

To get the information about the Soret lens formed in the sample due to the temperature gradient, we used the laser pulse

time interval $\Delta t = 20$ s and the following normalization for the transmittance:

$$T_N(z) = \frac{\Gamma(z,t = 20\ \text{s})}{\Gamma(z,t = 40\ \text{ms})}. \quad (5)$$

In this condition, introducing Eq. (4) into Eq. (5), we have

$$T_N(z) = \frac{1}{1 - 2\gamma\left(\frac{C_S}{1+\gamma^2}\right) + (1+\gamma^2)\left(\frac{C_S}{1+\gamma^2}\right)^2}. \quad (6)$$

Equation (6) will be used to fit the experimental data, and the Soret lens amplitude C_S will be obtained. As all the parameters present in Eq. (4), except S_T, are measured independently, the Soret coefficient is obtained. At each z position, five independent measurements of the transmittance are performed, and mean values are obtained.

V. RESULTS AND DISCUSSION

Following the method described above, the experimental curves for normalized transmittance $T_N(z)$ were obtained for the ferrofluids presented in Table I. Figure 2 shows two typical time-evolution normalized transmittance $\{T_N(t) = [I(z,t)]/[I(z,t = 40\ \text{ms})]\}$ curves used to build up the ZS transmittance curve (Fig. 3). All the ZS curves show a typical valley-to-peak shape, indicating that the matter (or Soret) lens has a self-focusing behavior (see Fig. 3). Since the sign of S_T is negative, the nanoparticles move to the hottest regions of the sample, typical of the thermophilic behavior. This result agrees with previous observations in similar magnetic colloids [7].

The Soret coefficient was obtained for all the ferrofluids, and its dependence with d_0 is shown in Fig. 4. A possible mechanism responsible for the thermophilic behavior observed in these materials is the decrease of the particles' surface charge in the hottest region of the samples illuminated by the Gaussian laser beam. This decrease of σ was observed in our potentiometric and conductometric experiments described above (see Fig. 1). The interaction between the electrostatically stabilized ferrofluid nanoparticles may be described by the Lennard-Jones-type potential, summing up the van der Waals and electrostatic potentials [32,33]. This kind of potential shows a characteristic equilibrium distance between particles, where the electrostatic and Van der Waals forces outweigh each other. If we consider the circular region of the sample irradiated by the Gaussian laser beam, and its induced temperature distribution, the surface charge of the particles should follow a similar behavior: particles in the center of the beam show σ_{sat} smaller than that of those in the borders of the beam. This implies that the equilibrium distance between the nanoparticles changes with temperature. The smaller the σ_{sat}, the smaller the electrostatic repulsion between particles, and the equilibrium distance between them decreases. As the sample experiences a temperature gradient when illuminated by the Gaussian

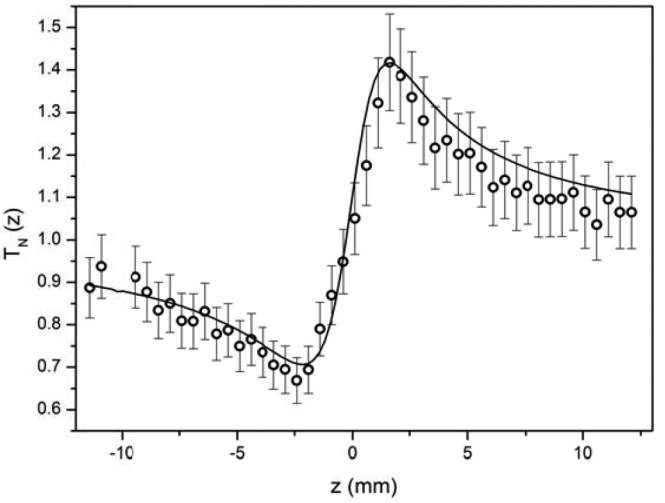

FIG. 3. Normalized transmittance as a function of z in the ZS experiment. Sample FF4. Solid curve is a fitting with Eq. (6).

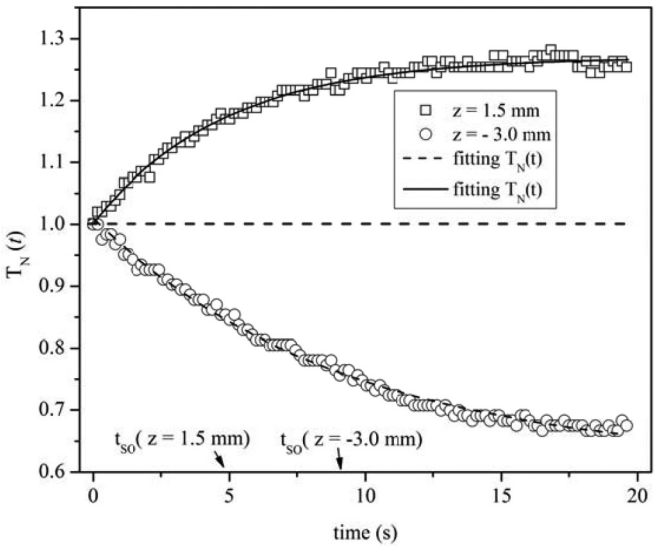

FIG. 2. Typical time-dependence normalized transmittance $[T_N(t)]$ curves, sample FF4, before ($z < 0$) and after ($z > 0$) the ZS lens focal point, during a laser pulse of $\Delta t = 20$ s.

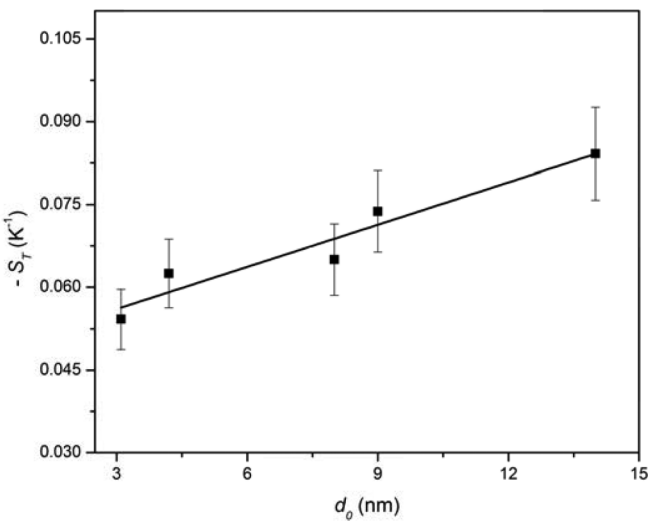

FIG. 4. Soret coefficient as a function of the particle diameter d_0. The solid line represents a linear fit.

beam, this implies a negative temperature gradient from the center of the sample to the borders, and a "gradient in the equilibrium distance" in the sense that the distance between particles is smaller in the hotter part of the sample and larger in the colder parts. This mechanism would be responsible for the nanoparticles' concentration gradient observed in our experiments, i.e., the negative sign of S_T, corresponding to the thermophilic behavior.

Let us discuss now the dependence of S_T with d_0 shown in Fig. 4. The tendency observed is that the bigger the particle, the larger the particles' concentration gradient for the same temperature gradient. To get the best functional dependence of S_T with d_0 present in our experimental data, we tested the fit quality (the R^2 parameter, i.e., the coefficient of determination) for the d_0 and d_0^2 dependences. The d (d_0^2) dependence gave $R^2 = 0.91$ ($R^2 = 0.88$). So, our results are best described by a linear dependence of S_T with the particle size, at least in the range of particle diameter investigated. A similar dependence was obtained in aqueous suspensions of polystyrene nanoparticles and proteins of T4 lysozyme and mutant variants of T4 lysozyme [21], and in water-in-oil microemulsion droplets [34]. The surface charge and the corresponding electrostatic Debye layer play an important role in thermodiffusion, and theoretical results, considering this influence, forecast a linear dependence of S_T with the particle's size [35,36]. It should be emphasized how difficult it is to obtain experimentally the size dependence of S_T without changing others parameters of the colloidal solution. On the other hand, some experimental results obtained with polystyrene beads reveal a different dependence, of the type $S_T \propto d_0^2$ and $D_T \propto d_0$ [11,20]. Braibanti and co-workers [22], however, showed that, at least in the case of polystyrene beads investigated by them, the thermophoretic mobility (or the thermal diffusion coefficient D_T) does not depend on the particle size. They argue that not only does the nature of the particle-solvent interface drive the particles diffusion, but there is also a striking relation between the interface, temperature, and particle size. Iacopini and co-workers [12] also reported experimental results from various macromolecular and colloidal systems showing that D_T does not depend on the particle size and that S_T is proportional to the particle size.

In the case of the magnetic colloids investigated in the present work, we assume that in our case D_T does not depend on d, and that $D_M = k_B T/(3\pi\eta d_H)$, where k_B, d_H, and η are the Boltzmann constant, the particle's hydrodynamic diameter (which is proportional to d_0), and the solution viscosity. The linear dependence of $S_T(D_T/D_M)$ found in our experiments (see Fig. 4) is straightforward. The angular coefficient of the best linear fit allows us to estimate the thermal diffusion coefficient $D_T = -1.9 \times 10^{-12}$ m^2/sK. A point that should be addressed is that, in the case of actual ferrofluids, particles are not monodisperse, presenting a log-normal distribution of diameters. In this case, the linear dependence of the Soret coefficient with d_0 discussed above has to be taken with caution when one analyzes the experimental results presented in Fig. 4. In fact, we may consider this dependence as a tendency that has to be encountered in the experimental determination of S_T as a function of d_0.

Let us now focus on the fluid medium where the nanoparticles are embedded. In addition to water, ions H^+ and NO_3^- are present to keep the solution neutral. To investigate the effect of the ionic strength of these ions on the thermodiffusion, we prepared samples of the FF1 solution with pH in the range from 3.3 to 1.0, and the Soret coefficients were measured. This range was chosen because there the particles' surface charge does not change significantly (see Fig. 1). It is important to note that only in some ranges of pH is it possible to stabilize a ferrofluid. For example, in the case shown in Fig. 1, for pH values above 3.5, the surface charge decreases and the ferrofluid changes from a stable sol to a metastable thyxotropic gel phase [37,38]. Figure 5(a) shows the result of S_T as a function of the pH of the solution. The Soret coefficient is higher for lower pH values, and it seems to reach a constant value at higher pH. Vigolo and co-workers [39] reported a dependence of the Soret coefficient with the ionic strength in micellar sodium dodecyl sulfate aqueous solutions by varying the concentration of NaOH in the medium. In this case, a change from thermophobic to thermophilic behavior for the

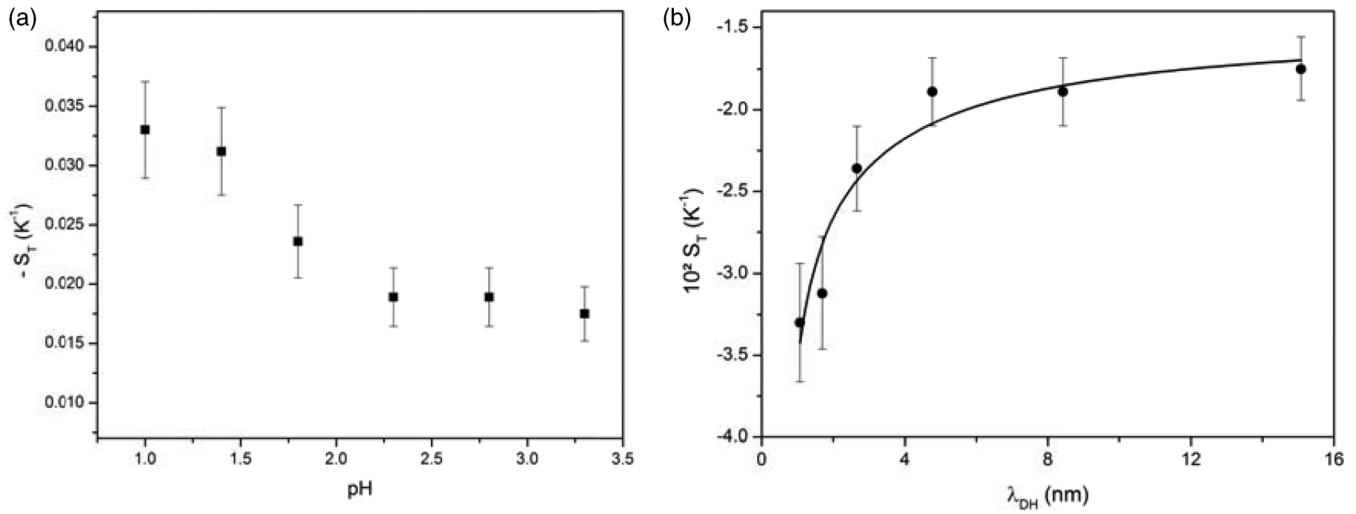

FIG. 5. (a) Soret coefficient as a function of the pH solution. Initial sample: FF1. (b) Soret coefficient as a function of the Debye-Hückel length (λ_{DH}). The solid line represents the best fit with Eq. (7) (Dhont's model).

micelles was observed with the salt addition. In our case, this inversion in the migration direction does not occur, at least in the range of pH investigated. The H^+ and NO_3^- ions have $S_T > 0$, moving to the colder regions of the sample, but H^+ has a much higher S_T value than that of NO_3^- [40]. At a given temperature gradient imposed by the Gaussian beam, a concentration gradient of H^+ and NO_3^- establishes in a way that a radial electric field is formed, pointing to the center of the illuminated region ($r = 0$). This electric field will push the positively charged nanoparticles to the hottest region of the samples ($r = 0$). This thermoelectric effect is more important for pH values smaller than 2.3. Similar behavior for many kinds of salts was reported by Eslahian [41] and explained by Majee [42], and the effect was associated with the electric field and changes in the zeta potential.

Since the diffusion coefficients of ions are larger than those of colloidal nanoparticles (typically 10^{-9} and 10^{-11} m^2/s, respectively), it is expected that ionic diffusion in a temperature gradient occurs much faster than the colloidal particle thermodiffusion [43]. Considering that our temperature gradient is low, the amplitude of the electric field, in the equilibrium, is given by $E = S\nabla T$, where S is the Seebeck coefficient showing the same profile as that of the temperature gradient [43]. The Seebeck coefficient is defined as [44] $S = k_B(\alpha_+ - \alpha_-)/e$, where α_+, α_-, are the ionic Soret parameters and e is the elementary charge. For common ions, the higher values of the Soret coefficient are those from hydrogenous ones (mainly H^+ and OH^-), and with the known values of these parameters [45], we found in our case $S = 0.22$ mV/K. Taking into account that the temperature gradient has a maximum value of 0.03 K/μm, the electric field may attain amplitudes around 6 V/m. A charged particle in this field has energy much higher than the thermal energy. So, in the ferrofluids investigated here, which have nitric acid, we can assume that the thermoelectric field has an influence on the nanoparticle thermodiffusion, which is increased with higher concentrations of H^+ ions.

Data shown in Fig. 5(a) may be presented as a function of the Debye-Hückel length (λ_{DH}), defined as $\lambda_{DH} = \sqrt{\varepsilon k_B T/(2c_0 e^2)}$, where ε is the electric permittivity of the solution (we used here that from water at $T = 23$ °C) and $c_0 = 2/10^{pH}$ (in mol/L). This plot [Fig. 5(b)] is particularly interesting because the Soret coefficient data as a function of λ_{DH} may be compared with theoretical predictions from Dhont's and Würger's models [46,47]. These models are based on the electrostatic contribution from the electric double layer only. Würger's model predicts a linear dependence of S_T with λ_{DH}, in the limit of $d \ll \lambda_{DH}$. He derived an expression for S_T as a function of λ_{DH} based on the electrostatic interactions between charged particles, considering the self-energy of them in the electrolyte medium, and the pair interaction potential [47]. This model is limited to the case of thin double layers, i.e., $d \ll \lambda_{DH}$. In our present experiment, $d \sim \lambda_{DH}$, and therefore this model is not appropriate to describe our experimental results. A more general expression for S_T as a function of λ_{DH}, valid for arbitrary Debye-Hückel lengths, was derived by Dhont [46] based on the temperature dependence of the reversible electrostatic work to build up the electric double layer around the nanoparticle. The equation, which expresses the λ_{DH} dependence of S_T, is given in Eq. (7),

$$S_T = \frac{1}{4T}\left(\frac{4\pi l_B^2 \sigma^*}{e}\right)^2 \frac{\kappa R}{(1+\kappa R)^2}\left(\frac{R}{l_B}\right)^3 \times \left\{1 - \frac{d\ln\varepsilon}{d\ln T}\left(1 + \frac{2}{\kappa R}\right)\right\} + \frac{1}{T}\left(\frac{4\pi l_B^2 \sigma^*}{e}\right)^2 \frac{1}{1+\kappa R}\left(\frac{R}{l_B}\right)^3 \frac{d\ln Q}{d\ln T} + A(T), \quad (7)$$

where $d\ln\varepsilon/d\ln T = -1.34$, $l_B = e^2/(4\pi\varepsilon k_B T)$ is the Bjerrum length (0.71 nm for water), $d\ln Q/d\ln T$ is the rate of surface-charge variation with temperature that in our case is -31 (from the results shown in Fig. 1), $\kappa = 1/\lambda_{DH}$, $R = d_0/2$, and $A(T)$ represents additional contributions from the core material and the solvation layer [3]. The parameter σ^* in Eq. (7) represents here the "effective charge density" of the particle. A similar approach was proposed by Piazza and Guarino [18]. The fit of Eq. (7) to the experimental data is shown in Fig. 5(b). The fitting parameters are $A(T) = -0.036$ K^{-1} and $\sigma^* = 0.02\sigma \approx 3.5 \times 10^{-3}$ C/m^2. This implies that the counterions efficiently screen the particle's surface charge.

VI. CONCLUSIONS

In summary, we have shown that in acidic ferrofluids, the Soret coefficient (S_T) increases with the particle's diameter, being best described by a functional dependence of the type $S_T \propto d_0$. The ZS technique and the generalization of the thermal lens model used experimentally to obtain the Soret coefficient values proved to be a reliable technique to measure S_T. An estimation of the temperature increasing during the ZS experiment guided potentiometric and conductometric experiments to the determination of the particle's surface charge. These results show that the surface charge decreases as the temperature increases, changing the electrostatic interaction between the nanoparticles. As a consequence, the particles get closer to each other in warmer regions when the Gaussian beam illuminates the sample. This generates a concentration gradient that creates the effect of a matter lens measured by the ZS technique. Increasing the ion concentration in samples of the FF1 mixture, we show that the thermoelectric field increases the particle's concentration gradient. This indicates that more than one physical mechanism is responsible for thermodiffusion in electrostatically stabilized ferrofluids.

ACKNOWLEDGMENTS

Financial support was provided by CNPq, CAPES, FAPESP, INCT, and NAP-FCx.

[1] Ch. Soret, Arch. Sci. Phys. Nat., Geneve **2**, 48 (1879).
[2] E. Ruckenstein, J. Colloid Interface Sci. **83**, 77 (1981).
[3] H. Ning, J. Dhont, and S. Wiegand, Langmuir **24**, 2426 (2008).
[4] S. Duhr, S. Aduini, and D. Braun, Eur. Phys. J. E **15**, 277 (2004).
[5] S. R. de Groot and P. Mazur, *Non-Equilibrium Thermodynamics* (North-Holland, Amsterdam, 1962).

[6] S. R. de Groot, *L'effet Soret—Diffusion Thermique dans les Phases Condensées* (North-Holland, Amsterdam, 1945).
[7] S. Alves, G. Demouchy, A. Bee, D. Talbot, A. Bourdon, and A. M. Figueiredo Neto, Philos. Mag. **83**, 2059 (2003).
[8] S. I. Alves, A. Bourdon, and A. M. Figueiredo Neto, J. Magn. Magn. Mater. **289**, 285 (2005).
[9] M. P. Santos, S. L. Gómez, E. Bringuier, and A. M. Figueiredo Neto, Phys. Rev. E **77**, 011403 (2008).
[10] P. Polyakov and S. Wiegand, Phys. Chem. Chem. Phys. **11**, 864 (2009).
[11] S. Duhr and D. Braun, Proc. Natl. Acad. Sci. (USA) **103**, 19678 (2006).
[12] S. Iacopini, R. Rusconi, and R. Piazza, Eur. Phys. J. E **19**, 59 (2006).
[13] Z. Wang, H. Kriegs, J. Buitenhuis, J. Dhont, and S. Wiegand, Soft Matter **9**, 8697 (2013).
[14] E. Bringuier and A. Bourdon, Phys. Rev. E **67**, 011404 (2003).
[15] R. E. Rosensweig, in *Ferrohydrodynamics* (Courier Dover, Mineola, New York, 1997).
[16] Q. A. Pankhurst, J. Connolly, S. K. Jones, and J. Dobson, J. Phys. D **36**, R167 (2003).
[17] G. Mériguet, G. Demouchy, E. Dubois, R. Perzynsky, and A. Bourdon, J. Non-Equilib. Thermodyn. **32**, 271 (2007).
[18] R. Piazza and A. Guarino, Phys. Rev. Lett. **88**, 208302 (2002).
[19] A. Mezulis, M. Maiorov, and E. Blums, J. Magn. Magn. Mater. **252**, 221 (2002).
[20] S. Duhr and D. Braun, Phys. Rev. Lett. **96**, 168301 (2006).
[21] S. A. Putnam, D. G. Cahill, and G. C. L. Wong, Langmuir **23**, 9221 (2007).
[22] M. Braibanti, D. Vigolo, and R. Piazza, Phys. Rev. Lett. **100**, 108303 (2008).
[23] S. Alves, A. Bourdon, and A. M. Figueiredo Neto, J. Opt. Soc. Am. B **20**, 713 (2003).
[24] F. A. Tourinho, R. Franck, and R. Massart, J. Mater. Sci. **25**, 3249 (1990).
[25] R. Aquino, F. A. Tourinho, R. Itri, M. C. F. L. Lara, and J. Depeyrot, J. Magn. Magn. Mater. **252**, 23 (2002).
[26] J. A. Gomes, M. H. Sousa, F. A. Tourinho, R. Aquino, G. J. Silva, J. Depeyrot, E. Dubois, and R. Perzynski, J. Phys. Chem. C **112**, 6220 (2008).
[27] C. Chenming and J. R. Whinnery, Appl. Opt. **12**, 72 (1973).
[28] A. F. C. Campos. F. A. Tourinho, G. J. da Silva, M. C. F. L. Lara, and J. Depeyrot, Eur. Phys. J. E **6**, 29 (2001).
[29] A. F. C. Campos, R. Aquino, F. A. Tourinho, F. L. O. Paula, and J. Depeyrot, Eur. Phys. J. E **36**, 42 (2013).
[30] S. Mustafa, B. Dilara, Z. Neelofer, A. Naeem, and S. Tasleem, J. Colloid Interface Sci. **204**, 284 (1998).
[31] J. R. Whinnery, Acc. Chem. Res. **7**, 225 (1974).
[32] P. C. Scholten, in *Colloid Chemistry of Magnetic Fluids in Thermomechanics of the Magnetic Fluids*, edited by B. Berkovski (Hemisphere, Bristol, 1978).
[33] J. N. Israelachvili, *Intermolecular and Surface Forces* (Academic, New York, 1991).
[34] D. Vigolo, G. Brambilla, and R. Piazza, Phys. Rev. E **75**, 040401 (2007).
[35] J. Anderson, Annu. Rev. Fluid Mech. **21**, 61 (1989).
[36] K. I. Morozov, *On the Theory of the Soret Effect in Colloids* (Springer-Verlag, Heidelberg, 2002).
[37] E. Hasmonay, A. Bee, J.-C. Bacri, and R. Perzynski, J. Phys. Chem. B **103**, 6421 (1999).
[38] A. F. C. Campos, E. P. Marinho, M. A. Ferreira, F. A. Tourinho, F. L. O. Paula, and J. Depeyrot, Braz. J. Phys. **39**, 230 (2009).
[39] D. Vigolo, S. Buzzaccaro, and R. Piazza, Langmuir **26**, 7792 (2010).
[40] J. N. Agar, C. Y. Mou, and J. L. Lin, J. Phys. Chem. **93**, 2079 (1989).
[41] K. A. Eslaihan, M. Maskos, and A. Coll, Sur. Phys. Eng. Asp. **413**, 65 (2012).
[42] A. Majee, Thèse de Doctorat, l'Université Bourdeaux 1, 2012.
[43] A. Majee and A. Würger, Soft Matter **9**, 2145 (2013).
[44] I. Chikina, V. Shikin, and A. A. Varlamov, Phys. Rev. E **86**, 011505 (2012).
[45] A. Würger, Phys. Rev. Lett. **101**, 108302 (2008).
[46] J. K. G. Dhont, S. Wiegand, S. Duhr, and D. Braun, Langmuir **23**, 1674 (2007).
[47] S. Fayolle, T. Bickel, and A. Würger, Phys. Rev. E **77**, 041404 (2008).